Preparation of Silica Nanosprings Using Cationic Gelators as Template

Yonggang Yang, Hiroaki Fukui, Masahiro Suzuki, Hirofusa Shirai, and Kenji Hanabusa*

Department of Functional Polymer Science, Faculty of Textile Science and Technology, Shinshu University, Ueda 386-8567

Received April 28, 2005; E-mail: hanaken@giptc.shinshu-u.ac.jp

Cationic cyclo(dipeptide) gelators **10mimClO$_4$**, **11mimClO$_4$**, and **11pyClO$_4$** were synthesized as templates for the sol–gel transcription reaction of alkoxysilanes. They were able to cause physical opaque gels in alcohols such as methanol, ethanol, and 1-propanol. Three-dimensional fibrous networks responsible for physical gelation were found in SEM images of gels. Sol–gel transcription reactions using the self-assemblies of three gelators as the templates were carried out in the presence of propylamine as a catalyst. When tetraethoxysilane (TEOS) was selected as a precursor, three kinds of morphologies, such as inner-helical nanotubes, right-handed nanobundles, and right-handed helical nanosprings were observed by electron microscopy. The helical nanosprings were preferentially formed as compared with nanotubes and nanobundles. On the other hand, the sol–gel polymerization of bis(triethoxysilyl)methane, 1,2-bis(triethoxysilyl)ethane, and 1,4-bis(triethoxysilyl)benzene as precursors gave nanoballs instead of tubular structures. When tetrabutylammonium fluoride (TBAF) was used as a catalyst, a helical tubular structure coated by silica nanoballs was identified.

Nanostructures, especially one-dimensional nanostructures such as wires, rods, belts, and tubes, could be used in many fields due to their electronic, optical, magnetic, and thermoelectric properties.[1] Both chemical and physical methods were designed to synthesize these nanostructures.[2] The helicity and periodicity of helical nanosprings, which belong to a new group of one-dimensional nanostructure, are of special interest for nano-engineering. Up to now, only a few papers have been published for the synthesis of nanosprings.[3] For example, the chemical vapor deposition (CVD) technique has been adopted to prepare nanosprings. Unfortunately, the yield of nanosprings was still low and the nanosprings were combined with other nanostructures; namely, the morphologies were not uniform.[3] It is of interest to create new methods and to find new ways for preparing nanosprings.

Helical structures can often be found in nature; for instance, α-helical polypeptides, double helical nucleic acids, spirulina, and spiral shells. With respect to artificial nanomaterials, helical nanowires, helical nanotubes,[4] inner helical nanotubes,[5] and hybrid helical bundles[6] have been prepared. Helical nanomaterials can be used as asymmetric reaction catalysts,[7] helical sensor,[8] and optical materials.[9] Generally, surfactants,[10] lipids,[11] and gelators[3,4] were selected as the templates for the preparation of these helical nanomaterials. It is thought that the templates act as structure-directing agents. Gelators are one of the candidates to act as templates, because they can show many kinds of morphologies; for example, rod, single helical strand, double helix, multiple helix, and twist ribbon.[12] And the sol–gel transcription method has been a promising method for the preparation of inner helical inorganic nanotubes.[13] In particular, chiral gelators have the potential to transfer their helicity and periodicity to the inorganic nanomaterials by using the sol–gel transcription method. In this paper, we report the preparation of silica nanosprings using cationic gelators as template.

Results and Discussion

Gelation Properties of Gelators 11pyClO$_4$, 10mimClO$_4$, and 11mimClO$_4$. Gelators **11pyClO$_4$**, **10mimClO$_4$**, and **11mimClO$_4$**, used as the templates, were synthesized by the pathway in Fig. 1. The compounds **11pyClO$_4$**, **10mimClO$_4$**, and **11mimClO$_4$** showed nearly the same gelation properties, being capable of gelling acetone, THF, and alcohols such as methanol, ethanol, 1-propanol, and *t*-butyl alcohol. Another notable property is that they can form transparent gels in water with less than 0.5 wt %. Because these gelators cause opaque gels in alcohols, CD spectra were taken using water as the solvent in which the transparent gels were formed. The CD

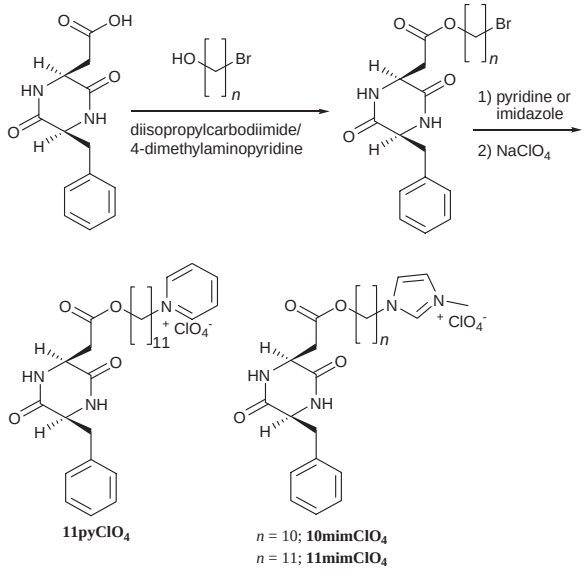

Fig. 1. Synthesis of gelators **11pyClO$_4$**, **10mimClO$_4$**, and **11mimClO$_4$**.

Published on the web October 31, 2005; DOI 10.1246/bcsj.78.2069

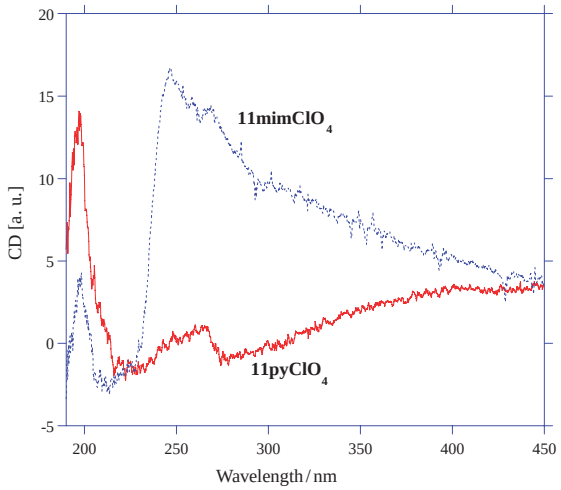

Fig. 2. CD spectra of the hydrogels of **11pyClO$_4$** and **11mimClO$_4$** (concentration: 5 mg/1.0 mL).

Fig. 3. FE-SEM image of xerogel prepared from *t*-butyl alcohol gels of **11pyClO$_4$** (concentration: 50 mg/0.5 mL).

spectra were strongly active as shown in Fig. 2. The source of the CD activity is unclear at this time, but it is assumed that the strong induced CD band originates from a chiral structure of gel aggregate. Furthermore, they are readily soluble in DMF, but insoluble in toluene and decane. To study visually the supramolecular self-assemblies of gelators, we used FE-SEM. Almost resembling morphologies were observed for the three gelators. Figure 3 shows the SEM image of the xerogel obtained from *t*-butyl alcohol gel of **11pyClO$_4$** by the freeze-and-pump method. We can detect two kinds of nanofibers; namely, one is huge nanofibers which are uniform in diameter (600–400 nm) and the other is fine nanofibers whose diameter is around 50 nm. Unfortunately, it was difficult to decide the helicity of their fibers from the SEM image of Fig. 3, although they were built up by chiral compounds.

Formation of Silica Nanosprings Using Propylamine as Catalyst. Figures 4 and 5 show the FE-SEM images of the silica obtained by the sol–gel polymerization of TEOS by the transcription method using gelator **10mimClO$_4$**. Figure 6 shows SEM images of the silica that were obtained using the self-assemblies of **11mimClO$_4$** and **11pyClO$_4$** as templates. There are almost the same morphologies in the three silica obtained by replication of **10mimClO$_4$**, **11mimClO$_4$**, and **11pyClO$_4$**. Namely, we can recognize three kinds of

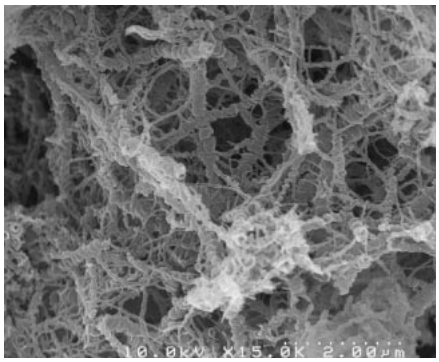

Fig. 4. FE-SEM image of silica obtained by sol–gel transcription method using gelator **10mimClO$_4$**.

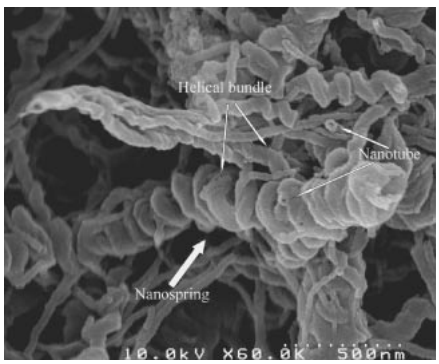

Fig. 5. FE-SEM image of silica obtained by sol–gel transcription method using gelator **10mimClO$_4$**.

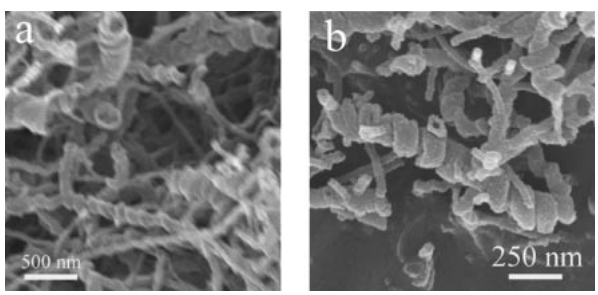

Fig. 6. FE-SEM images of silica obtained by sol–gel transcription method using gelators **11mimClO$_4$** (a) and **11pyClO$_4$** (b).

morphologies building up a hierarchical structure. The first morphology is helical *nanotubes* with an inner diameter around 10–40 nm. These nanotubes possess an inner helical structure (Fig. 5 and Fig. 7b). The second morphology is right-handed helical *nanobundles* which are constructed by gathering nanotubes (Fig. 5). The diameters of helical nanobundles are around 100 nm. The third morphology is the most interesting *nanosprings*. Many right-handed helical nanosprings with a diameter around 300 nm were constructed by right-handed helical nanobundles in these silica (Fig. 4, Fig. 5, and Fig. 6). The inner diameters of nanosprings were around 100 nm. The TEM image of nanosprings looks complicated, but we confirmed they possess helical and tubular structures (Fig. 7a). These morphologies, from nanotube to right-handed nanospring via right-handed helical nanobundle, can

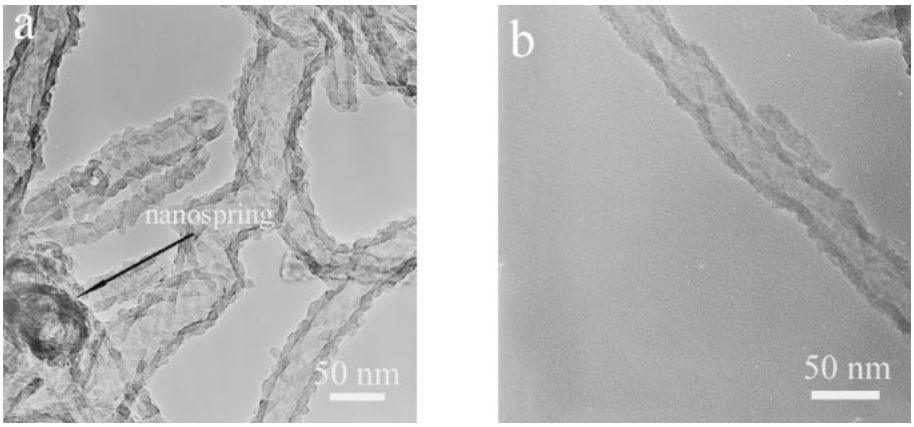

Fig. 7. TEM images of the silica obtained by sol–gel transcription method using gelators (a) **11mimClO$_4$** and (b) **10mimClO$_4$**.

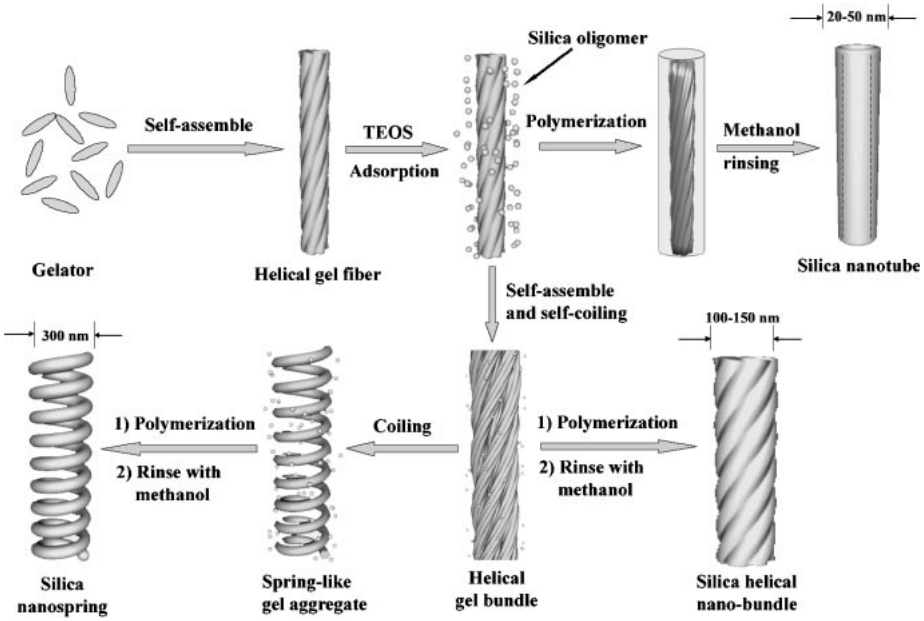

Fig. 8. The formation of inner-helical silica tube, helical silica bundle, and silica nanospring.

help us not only to understand the hierarchical structure of self-assembly of gelators during the sol–gel transcription process, but also to understand that the morphologies of the self-assembly formed by gelators were sensitively influenced by surroundings such as solvents, catalyst, and TEOS. From the comparison of Fig. 3 and Fig. 4, it is thought that the helicity and periodicity of the self-assemblies of gelators are amplified during the sol–gel transcription process.

The postulated mechanism of the formation of nanotubes, helical nanobundles, and nanosprings is shown in Fig. 8. First of all, helical gel fibers are constructed through the self-assembly of gelators. Secondly, silica oligomers are adsorbed on the surfaces of the helical gel fibers. At the same time the helical gel bundles are constructed by these fibers and spring-like gel aggregates are formed by the self-assembly and self-coiling of the helical gel bundles. The sol–gel polymerization of TEOS oligomers proceeds on the surface of the helical gel fibers, helical gel bundles, and spring-like gel aggregates side by side. After the polymerization is completed, gelators are removed by washing with hot methanol. Finally, helical nanotubes, helical nanobundles, and nanosprings of silica are constructed. Although the silica nanosprings were combined with nanotubes and helical nanobundles, the nanosprings were preferentially formed (Fig. 4). If we carefully select appropriate gelators and reaction conditions, we can probably produce pure nanosprings. Considering that the gelators show a variety of morphologies, the sol–gel polymerization method using them as templates should be a powerful method for the synthesis of nano materials.

Formation of Hybrid Silica Nanoparticles. The research of hybrid silica has been developing rapidly from the periodic mesoporous materials with organic segments in the walls[14] to hybrid nanofibers.[6] The organic segments in hybrid silica can improve the mechanical properties. We studied the sol–gel transcription of bis(triethoxysilyl)methane, 1,2-bis(triethoxysilyl)ethane, and 1,4-bis(triethoxysilyl)benzene as the precursors. In the case of the sol–gel transcription of bis(triethoxysilyl)methane using the gelator **11pyClO$_4$** as a template, short

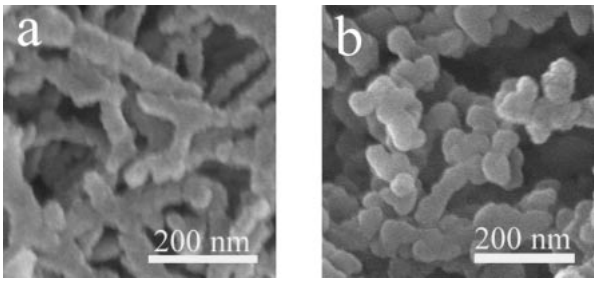

Fig. 9. FE-SEM images of hybrid silica obtained by sol–gel polymerization of bis(triethoxysilyl)methane (a) and 1,2-bis(triethoxysilyl)ethane (b) using gelator **11pyClO$_4$**.

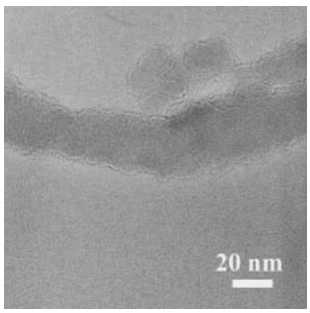

Fig. 10. TEM image of hybrid silica obtained by sol–gel polymerization of bis(triethoxysilyl)methane using gelator **11pyClO$_4$**.

clusters tying in a row were obtained (Fig. 9a), however, the clusters possessed no inner structure (Fig. 10). With respect to 1,2-bis(triethoxysilyl)ethane, only nanoballs tying in a row were found (Fig. 9b). These hybrid nanoballs are several tens of nanometers in diameter. The sol–gel transcription of 1,4-bis(triethoxysilyl)benzene gave the cotton-like hybrid silica, however, it shrank into nonporous transparent small particles during the air-drying procedure. Although we do not succeed in preparing tubular structures with the sol–gel transcription of silsesquioxanes as precursors as yet, it is interesting to note that the particles could be controlled in nano-size (less than 50 nm),[15] which can increase the surface area of hybrid silica.

Formation of Tubular Structures Using TBAF as Catalyst. We attempted to prepare silica with tubular structure by the sol–gel polymerization of TEOS using TBAF as the catalyst instead of propylamine. Figure 11 shows FE-SEM and TEM images of silica obtained by sol–gel polymerization of TEOS in the presence of TBAF using gelator **11mimClO$_4$**. Right-handed helical silica nanotubes, whose surface was coated with nanoparticles, were identified. The diameters of nanoparticles were less than 10 nm. The inner diameters of the nanotubes are around 30 nm. Because when TBAF was used as catalyst, the polymerization speed of TEOS was very fast, so many nanoparticles were identified. Furthermore, when the concentration of TBAF was increased, only silica balls were obtained.

Conclusion

Three cationic gelators, synthesized as templates for sol–gel polymerization, formed huge nanofibers and fine nanofibers whose diameters are ca. 500 nm and ca. 50 nm in gels. Three

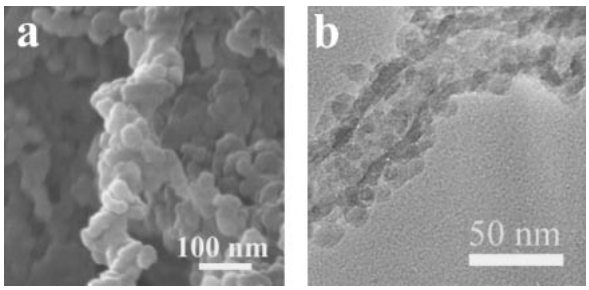

Fig. 11. FE-SEM (a) and TEM (b) images of silica obtained by sol–gel polymerization of TEOS in the presence of TBAF using gelator **11mimClO$_4$**.

kinds of morphologies were observed in the silica obtained from TEOS. They were helical nanotubes, right-handed nanobundles, and right-handed helical nanosprings. The helical nanosprings were preferentially formed as compared with others. Sol–gel polymerization with bis(triethoxysilyl)-methane, 1,2-bis(triethoxysilyl)ethane, and 1,4-bis(triethoxysilyl)benzene as precursors gave nanoballs instead of tubular structures. When TBAF instead of propylamine was used as a catalyst, a helical tubular structure coated by silica nanoballs was identified.

Experimental

Chemicals. The perchlorate salts, **11pyClO$_4$**, **10mimClO$_4$**, and **11mimClO$_4$**, were obtained by ionic exchange[16] between sodium perchlorate and the corresponding bromide salts which were synthesized according to the literature.[17] Cyclo(L-asparaginyl-L-phenylalanyl) was prepared by cyclization of L-asparaginyl-L-phenylalanine methyl ester.[18]

Cyclo(L-β-11-bromoundecylasparaginyl-L-phenylalanyl). Cyclo(L-asparaginyl-L-phenylalanyl) (10.23 g, 0.039 mol) was dissolved in 250 mL of DMF, and then 4-dimethylaminopyridine *p*-toluenesulfonate (17.22 g, 0.059 mol), 11-bromo-1-undecanol (10.00 g, 0.039 mol), and diisopropylcarbodiimide (5.83 g, 0.046 mol) were added. The solution was stirred at room temperature overnight. After evaporating DMF under reduced pressure, the residue was washed with water. The crude product was recrystallized from a mixture of methanol and diethyl ether. Cyclo(L-β-11-bromoundecylasparaginyl-L-phenylalanyl) was obtained in a yield of 13.9 g (72%).

***N*-Methylimidazolium Bromide Salt of Cyclo(L-asparaginyl-L-phenylalanyl) Derivative (11mimBr).** A mixture of cyclo(L-β-11-bromoundecylasparaginyl-L-phenylalanyl) (5.95 g, 12 mmol) and *N*-methylimidazole (5 mL, 62.5 mmol) in DMF (30 mL) was heated at 60 °C for 24 h under a nitrogen atmosphere. After the solvent was removed in vacuum, the residue was dissolved in 50 mL of methanol. Diethyl ether was added dropwise to the solution until the cloudy endpoint was reached. The solution was cooled at 0 °C, and then the precipitate was filtered and dried. Yield: 6.10 g (88%).

***N*-Methylimidazolium Perchlorate Salt of Cyclo(L-asparaginyl-L-phenylalanyl) Derivative (11mimClO$_4$).** To 50 mL of saturated sodium perchlorate aqueous solution, the aqueous solution of **11mimBr** (2.00 g, 3.46 mmol) was added under stirring. After the mixture was stirred for 12 h, the precipitate was filtered, washed with distilled water and dried. The crude product was recrystallized from a mixture of methanol and diethyl ether. Yield 1.96 g (95%). ^{1}H NMR (400 MHz, DMSO): δ 1.26–2.0 (18H, m,

CH_2), 2.92 (2H, d, CH_2Ph), 3.10 (2H, d, CH_2COO), 3.84 (3H, s, CH_3), 3.92 (2H, t, CH_2O), 4.03 (1H, t, $CH(PhCH_2)$), 4.14 (2H, t, CH_2-methylimidazole), 4.22 (1H, t, $CH(CH_2COO)$), 7.17–7.28 (5H, m, Ar), 7.69 (1H, s, NCH), 7.75 (1H, s, NCH), 7.97 (1H, s, NH), 8.17 (1H, s, NH), 9.08 (1H, s, NCHN). Elemental analysis calcd (%) for $C_{28}H_{41}ClN_4O_8$ (596.26): C, 56.32; H, 6.92; N, 9.38%. Found: C, 56.03; H, 6.73; N, 9.35%.

***N*-Methylimidazolium Perchlorate Salt of Cyclo(L-asparaginyl-L-phenylalanyl) Derivative (10mimClO$_4$).** ^{1}H NMR (400 MHz, DMSO): δ 1.26–2.0 (16H, m, CH_2), 2.92 (2H, d, CH_2Ph), 3.10 (2H, d, CH_2COO), 3.84 (3H, s, CH_3), 3.92 (2H, t, CH_2O), 4.03 (1H, t, $CH(PhCH_2)$), 4.14 (2H, t, CH_2-methylimidazole), 4.22 (1H, t, $CH(CH_2COO)$), 7.17–7.28 (5H, m, Ar), 7.69 (1H, s, NCH), 7.75 (1H, s, NCH), 7.97 (1H, s, NH), 8.17 (1H, s, NH), 9.08 (1H, s, NCHN). Elemental analysis calcd (%) for $C_{27}H_{39}ClN_4O_8 \cdot H_2O$ (601.09): C, 53.95; H, 6.88; N, 9.32%. Found: C, 53.27; H, 6.17; N, 9.08%.

***N*-Pyridinium Bromide Salt of Cyclo(L-asparaginyl-L-phenylalanyl) Derivative (11pyBr).** Cyclo(L-β-11-bromoundecylasparaginyl-L-phenylalanyl) (5.95 g, 12 mmol) was heated in 100 mL of pyridine at 90 °C overnight under a nitrogen atmosphere. After evaporating pyridine, the recrystallization from a mixture of methanol and diethyl ether gave **11pyBr** in a yield of 5.97 g (84%).

***N*-Pyridinium Perchlorate Salt of Cyclo(L-asparaginyl-L-phenylalanyl) Derivative (11pyClO$_4$).** To 50 mL of saturated sodium perchlorate aqueous solution, the aqueous solution of **11pyBr** (2.00 g, 3.48 mmol) was added under stirring. After the mixture was stirred for 48 h, the precipitate was filtered, washed with distilled water and dried. The recrystallization from a mixture of methanol and diethyl ether gave **11pyClO$_4$** in a yield of 1.65 g (80%). Compound **11pyClO$_4$**: ^{1}H NMR (400 MHz, DMSO): δ 1.25–2.0 (18H, m, CH_2), 2.92 (2H, d, CH_2Ph), 3.10 (2H, d, CH_2COO), 3.92 (2H, t, CH_2O), 4.03 (1H, t, $CH(PhCH_2)$), 4.22 (1H, t, $CH(CH_2COO)$), 4.59 (2H, t, CH_2N), 7.17–7.28 (5H, m, Ar), 7.97 (1H, s, NH), 8.16 (1H, s, NH), 8.17 (2H, m, CH), 8.60 (1H, t, CH), 9.08 (2H, d, NCH). Elemental analysis calcd (%) for $C_{29}H_{40}ClN_3O_8$ (594.10): C, 58.63; H, 6.79; N, 7.07%. Found: C, 57.84; H, 6.48; N, 6.95%.

Sol–Gel Polymerization. The typical procedure of the sol–gel polycondensation of TEOS using propylamine as a catalyst was carried out as follows. Fifty seven mg of gelator **11pyClO$_4$**, 10 μL of H_2O, 42 μL of TEOS, and 10 μL of propylamine were dissolved in 0.50 mL of ethanol to form a transparent solution by heating. After being cooled down with an ice-water bath, the reaction mixture was kept at room temperature for 7 days under static conditions. Finally, the gelator **11pyClO$_4$** was removed by washing with methanol and then dried in the air overnight. In order to transfer the morphologies of gelators to organic/inorganic hybrid silica, we performed the sol–gel polycondensation of bis(triethoxysilyl)methane, 1,2-bis(triethoxysilyl)ethane, and 1,4-bis(triethoxysilyl)benzene. Consequently the hybrid silica were obtained by the similar procedure described for TEOS.

The typical procedure for the sol–gel polycondensation of TEOS using TBAF as the catalyst is as follows. Gelator **11mimClO$_4$** (30 mg), 10 μL of TBAF aq (0.05 M), and 42 μL of TEOS were dissolved in 0.30 mL of *t*-butanol to form a transparent solution. After being cooled down with an ice-water bath to form an opaque gel, the reaction mixture was kept at room temperature for 7 days under static conditions. Finally, the gelator **11mimClO$_4$** was removed by washing with methanol and then dried in air overnight.

Characterization. Transmission electron microscope (TEM) images were obtained using a JEOL JEM-2010. Field emission scanning electron microscopy (FE-SEM) was taken on a Hitachi S-5000. Circular dichroism (CD) spectra were measured on a JASCO J650 spectrophotometer (cell diameter 0.1 mm). ^{1}H NMR spectra were recorded with a Bruker AVANCE 400 spectrometer using TMS as an internal standard. Elemental analyses were performed on a Perkin-Elmer series II CHNS/O analyzer 2400.

This work was supported by Grant-in-Aid for 21st Century COE Program and a grant (No. 15350132) by the Ministry of Education, Culture, Sports, Science and Technology of Japan.

References

1 Y. Xia, P. Yang, Y. Sun, Y. Wu, B. Mayer, B. Gates, Y. Yin, F. Kim, and H. Yan, *Adv. Mater.*, **15**, 353 (2003).

2 T. Yamamoto, H. Yin, Y. Wada, T. Kitamura, T. Sakata, H. Mori, and S. Yanagida, *Bull. Chem. Soc. Jpn.*, **77**, 757 (2004); A. Habib, M. Tabata, and Y. G. Wu, *Bull. Chem. Soc. Jpn.*, **78**, 262 (2005).

3 H.-F. Zhang, C.-M. Wang, E. C. Buck, and L.-S. Wang, *Nano Lett.*, **3**, 577 (2003).

4 J. H. Jung, Y. Ono, K. Hanabusa, and S. Shinkai, *J. Am. Chem. Soc.*, **122**, 5008 (2000); J. H. Jung, Y. Ono, and S. Shinkai, *Chem.—Eur. J.*, **6**, 4552 (2000); J. H. Jung, H. Kobayashi, M. Masuda, T. Shimizu, and S. Shinkai, *J. Am. Chem. Soc.*, **123**, 8785 (2001); S. Kobayashi, N. Hamasaki, M. Suzuki, M. Kimura, H. Shirai, and K. Hanabusa, *J. Am. Chem. Soc.*, **124**, 6550 (2002); J. H. Jung, Y. Ono, and S. Shinkai, *Chem.—Eur. J.*, **6**, 4552 (2000); K. Sugiyasu, S. Tamaru, M. Takeuchi, D. Berthier, I. Huc, R. Oda, and S. Shinkai, *Chem. Commun.*, **2002**, 1212; J. H. Jung, K. Yoshida, and T. Shimizu, *Langmuir*, **18**, 8724 (2002).

5 J. H. Jung, S. Shinkai, and T. Shimizu, *Chem. Mater.*, **15**, 2141 (2003).

6 J. J. E. Moreau, L. Vellutini, M. Wong Chi Man, and C. Bied, *J. Am. Chem. Soc.*, **123**, 1509 (2001); Y. Yang, M. Nakazawa, M. Suzuki, M. Kimura, H. Shirai, and K. Hanabusa, *Chem. Mater.*, **16**, 3791 (2004); B. Boury and R. J. P. Corriu, *Chem. Commun.*, **2002**, 795.

7 K. Soai, S. Osanai, K. Kadowaki, S. Yonekubo, T. Shibata, and I. Sato, *J. Am. Chem. Soc.*, **121**, 11235 (1999).

8 K. Bodenhöfer, A. Hierlemann, J. Seemann, G. Gauglitz, B. Koppenhoefer, and W. Gpel, *Nature*, **387**, 577 (1997).

9 I. Hodgkinson and Q. H. Wu, *Adv. Mater.*, **13**, 889 (2001).

10 S. Che, Z. Liu, T. Ohsuna, K. Sakamoto, Q. Terasaki, and T. Tatsumi, *Nature*, **429**, 281 (2004).

11 A. M. Seddon, H. M. Patel, S. L. Burkett, and S. Mann, *Angew. Chem., Int. Ed.*, **41**, 2988 (2002).

12 K. J. C. van Bommel, A. Friggeri, and S. Shinkai, *Angew. Chem., Int. Ed.*, **42**, 980 (2003); K. Hanabusa, M. Yamada, M. Kimura, and H. Shirai, *Angew. Chem., Int. Ed.*, **35**, 1949 (1996).

13 Y. Ono, K. Nakashima, M. Sano, Y. Kanekiyo, K. Inoue, J. Hojo, and S. Shinkai, *Chem. Commun.*, **1998**, 1477.

14 T. Asefa, M. J. MacLachlan, N. Coombs, and G. A. Ozin, *Nature*, **402**, 867 (1999); S. Inagaki, S. Guan, T. Ohsuna, and O. Terasaki, *Nature*, **416**, 304 (2002).

15 J. E. Haskouri, D. O. de Zárate, C. Guillem, A. Beltrán-Porter, M. Caldés, M. D. Marcos, D. Beltrán-Porter, J. Latorre, and P. Amorós, *Chem. Mater.*, **14**, 4502 (2002).

16 M. Suzuki, S. Owa, M. Yumoto, M. Kimura, H. Shirai, and

K. Hanabusa, *Tetrahedron Lett.*, **45**, 5399 (2004); M. Suzuki, S. Owa, M. Yumoto, M. Kimura, H. Shirai, and K. Hanabusa, *Tetrahedron Lett.*, **46**, 303 (2005).

17 Y. Yang, M. Suzuki, M. Kimura, H. Shirai, and K. Hanabusa, *Chem. Commun.*, **2004**, 1332.

18 K. Hanabusa, M. Matsumoto, M. Kimura, A. Kakehi, and H. Shirai, *J. Colloid Interface Sci.*, **224**, 231 (2000).